

Theon:

A proposal to the M8 launch slot of ESA's Voyage 2050 program, for the spectroscopic exploration of the UV and VIS universe

Frank Grupp^{a,b}, Renyu Hu^c, Hanna Kellermann^a, Helena Lamprecht^a, Sara Seager^{d,e,f}, and Kevin Heng^{a,g,h}

^aUniversity Observatory Munich, Ludwig-Maximilians-Universität, Scheinerstr. 1, 81679
Munich, Germany

^bMax-Planck-Institut für extraterrestrische Physik, Giessenbachstr. 1, 85748 Garching,
Germany

^cJet Propulsion Laboratory, California Institute of Technology, Pasadena, CA 91109, USA

^dDepartment of Earth, Atmospheric and Planetary Sciences, Massachusetts Institute of
Technology, 77 Massachusetts Avenue, Cambridge, MA 02139, USA

^eDepartment of Physics, Massachusetts Institute of Technology, 77 Massachusetts Avenue,
Cambridge, MA 02139, USA

^fDepartment of Aeronautics and Astronautics, Massachusetts Institute of Technology, 77
Massachusetts Avenue, Cambridge, MA 02139, USA

^gUniversity of Warwick, Department of Physics, Astronomy & Astrophysics Group, Coventry
CV4 7AL, UK

^hUniversity College London, Department of Physics & Astronomy, Gower St, London, WC1E
6BT, UK

ABSTRACT

"Theon" is our answer to ESA's M8 call for a medium-class launch slot in 2041. It provides capabilities of ultraviolet (UV) and visible (VIS) spectroscopy with a spectral resolution of $R \approx 100,000$. Light is collected by a 2-meter class ultralight-weighted Gregorian telescope. A deformable secondary mirror will correct residual deviations from the g-release modeling and in-orbit reality.

Theon will host a suite of three instruments that allow high-resolution spectroscopy in the $1000 \dots 2000 \text{ \AA}$ and the $2000 \dots 8000 \text{ \AA}$ regimes. A low-resolution spectrograph with an R of $5 \dots 150$ between 200 and 900 nm complements the instrumental setup. A fourth instrument could be a student-built 900 nm to $1.4 \mu\text{m}$ spectrophotometer. Besides a strong educational aspect, this would complement existing and planned missions on the ground and in space.

The low spectral resolution instrument is built for the rendezvous option (Theon*), where Theon flies in formation with a starshade.¹

Both mission parts, Theon and Theon*, serve a broad variety of science cases grouped around three science pillars: *Exoplanets and their host stars, inflows and outflows of the local baryon cycle*, and the *evolution of galaxies*. The mission is planned to be flown in the outer Lagrange point L2 of the Sun-Earth system, a mission lifetime is planned to be 6 years minimum, with an extension of another 3 + 3 years possible.

Our low-resolution spectrograph, which is designed for maximum throughput and optimized for the starshade science case, can serve as a pathfinder and technology and science verification platform for the Habitable Worlds Observatory (HWO).^{2,3}

Keywords: Habitable Worlds Observatory, starshade, Theon, UV Spectroscopy, Hubble Space Telescope, active optics, space telescope, wave front correction, ESA, NASA

Further author information: (Send correspondence to F. G.)

F. G.: E-mail: frank.grupp@lmu.de, Telephone: +49 171 316 5843, Zoom: frank.grupp@lmu.de

1. INTRODUCTION

With the Hubble Space Telescope⁴ nearing its end of life, there is no large space telescope of high spectral resolution planned for the ultraviolet and visible light regime for orbit in the 2030s to 2040s. At the same time, the scientific need for high-resolution spectroscopic observation is increasing. In particular, this includes the exploration of other worlds - such as faint point sources or planets - that either transit in front of their host stars or appear alongside them as point sources up to 100 billion times dimmer than their central star. Theon and Theon* are sized by two science cases: *Exoplanet transit spectroscopy* and *diffuse circumgalactic medium*.

In the following, we will briefly present these science cases within the key pillars of the mission concept.

1.1 Science pillars of the mission

The key science pillars form the scientific framework of the mission. As a general-purpose observatory, a significant fraction of up to 40 % of the observation time will be allocated to guest observer programs, distributed on an application basis among observing projects of varying sizes.

Exoplanets and their host stars: detect carbon, oxygen, and other metals in the upper atmospheres of small exoplanets (super-Earths and sub-Neptunes), establish UV profiles of their host stars, and measure bulk compositions of rocky exoplanets via observing debris-polluted white dwarfs, magnetospheres of solar system planets and moons.

This first pillar focuses on small exoplanets (super-Earths and sub-Neptunes) between the sizes of Earth and Neptune, which are commonly found around other stars.⁵ UV spectroscopy probes carbon, hydrogen, oxygen, nitrogen, and metals in their upper atmospheres (exospheres), which are important tracers of planetary geology. The UV cross sections are several orders of magnitude higher compared to the optical or infrared, which enables smaller exoplanets to be probed more decisively (i.e., via much deeper transit depths). The high spectral resolution is crucial for resolving the individual spectral lines, which will usher in the era of high-precision atmospheric chemistry of exoplanets from space. The UV range of wavelengths is completely inaccessible from the ground. Placing the spectrograph in space allows for absolute chemical abundances to be measured accurately due to the absence of confusion from the atmosphere of Earth (telluric absorption). Access to Lyman-alpha ($\approx 120 \text{ nm}$) at high spectral resolution allows for the measurement of stellar winds that drive mass loss and the evolution of exoplanetary atmospheres. Spectroscopy at high resolution enables the reconstruction of the stellar UV profiles, which are critical for understanding planetary photochemistry and atmospheric escape. In the Solar System, UV spectral lines of H, O, and H₂O trace the mass flows from potentially habitable satellites to the magnetospheric environments of the gas plane.

Inflows and outflows of the local baryon cycle: measure composition and structure of inflows/outflows from the interstellar medium (ISM), protoplanetary disks, massive stars, compact binaries.

The second pillar includes the study of the ISM and protoplanetary disks, where the raw materials for new stars and the earliest phases of the planet-formation process can only be fully characterized with UV spectroscopy. Detailed studies of the local ISM, as well as the transition to the dense phases of the ISM where molecules become abundant, require spectral resolutions of $\sim 100,000$ to disentangle the velocity structure of the solar neighborhood,⁶ measure unsaturated spectral features, and resolve the rotational temperature structure of interstellar molecules.⁷ The combination of wide spectral coverage and high resolution enables the measurement of fundamental physical properties of the ISM, such as chemical and molecular abundances, temperature, turbulence, ionization, and dust content.⁸

After the interstellar gas and dust have collapsed to a protoplanetary disk, UV absorption line spectroscopy provides direct characterization of key atomic and molecular species (e.g., H, C, N, O, CO, H₂O), including the dominant mass component of the disk (molecular hydrogen or H₂⁹), providing absolute abundance measurements without having to rely on molecular conversion factors or geometry dependent model results inherent to emission line observations.¹⁰ At the same time, H₂ fluorescence at high resolution provides a sensitive probe of the molecular disk winds that may be responsible for angular momentum transfer during the final stages of star and planet formation. UV spectroscopy is also critical for the study of the more

diffuse ISM on larger scales, where the narrow absorption lines of neutral and ionized species (e.g., HI, OI, KrI, CII, FeII, NiII, SiII, and many others) allow the detailed study of the chemical and physical properties of the gas.^{11,12} With its high resolution ($R \sim 100,000$), Theon will be key to measuring the chemical and kinematical properties of individual groups of neutral ISM clouds and unveil ISM complexity, bridging the small and large scales in our Galaxy.

The chemical evolution of our Galaxy is driven by both massive stars and compact binaries, enriching their environments by strong stellar winds and their end-of-life supernova explosions.¹³ Many stars are born in tight binary systems,¹⁴ but our understanding of their evolution remains incomplete.¹⁵ Compact binaries hosting white dwarfs serve as astrophysical probes to constrain models of binary evolution. From white dwarf masses, chemical abundances, accretion and rotation rates, it is possible to reconstruct the formation, evolution, and final fate of the binary,¹⁶ the latter being intimately linked to thermonuclear supernovae. Detached double white dwarfs are particularly relevant as they can give rise to a supernova by spiraling in under the effect of gravitational radiation until they finally merge. High-resolution spectroscopy across the $1000 - 8000 \text{ \AA}$ range is fundamental to detect these binaries via radial velocity variations in the narrow core of the Balmer lines.¹⁷ Double-white dwarf systems are among the brightest sources of low-frequency gravitational waves in our Galaxy.¹⁸ Understanding the properties of the evolution of compact binaries is critically important in the context of the low-frequency gravitational wave signals that ESA's Laser Interferometer Space Antenna (LISA) mission will detect.¹⁹ Thus, there is a major scientific connection between Theon and LISA.

Evolution of galaxies: measure composition and gas-phases of the circumgalactic medium (CGM) and intergalactic medium (IGM) of local and distant galaxies and the Lyman-alpha forest as constraints on the evolution of galaxies.

The third pillar focuses on gas around and between galaxies, the CGM and IGM, which play a key role in the evolution of galaxies.^{20,21} The characteristic temperature and density of the outflowing and infalling gas place the key spectral diagnostics in the rest-frame UV spectral window.²² Only high-resolution UV spectroscopy can access this gas in low-to-intermediate redshift galaxies, where the angular resolution is sufficient to study the feedback cycle between massive stars, supernovae, and gas-phase physics in detail. Previous observations and galactic evolution simulations have shown that a spectral resolution of $\sim 100,000$ and a sensitive optical system are required for resolving individual velocity components and line profiles in diffuse galactic halos.²³ This capability is essential for understanding the interaction of this gas with the IGM. High-resolution spectroscopy from UV to optical wavelengths enables us to quantify the Lyman-alpha forest with redshift and thereby constrain the UV background that keeps the intergalactic gas ionized²⁴ over 90 % of the history of the universe.

1.2 Observation and science requirements

From the science pillars above, a number of key observational requirements are defined. Those are presented in Table 1. This is the very first set of observational requirements, and it will be extended and refined along the mission proposal process.

Table 1. Selected scientific objectives of the Theon mission (non-exhaustive list).

Scientific Objective	Targets	Scientific Outcomes / Products
Upper atmospheres of small exoplanets	~ 50 super-Earths, sub-Neptunes and Neptunes	Detections of hydrogen, carbon, oxygen, nitrogen and metals as probes of atmospheric escape.
UV properties of exoplanet host stars	~ 100 exoplanet host stars, including ~ 10 ultracool dwarfs	Reconstruct UV profiles (as inputs for atmospheric photochemistry and escape of exoplanets), tomography of stellar surfaces, monitor stellar flares.
Demographics of white dwarf enrichment	~ 200 white dwarfs	Bulk abundances of a wide range of exoplanetary bodies.
Properties of interstellar medium	~ 500 sightlines	Gas temperature, composition, velocity, ionization state, dust content, level of turbulence, and gas mixing.
Three-dimensional structures of protoplanetary disks	~ 100 protoplanetary disks	Direct measurement of composition and temperatures of inner disks; atomic and molecular disk winds.
Binary evolution and supernova progenitors	~ 500 compact binaries hosting white dwarfs (including mass-exchanging and detached systems)	Accurate white dwarf parameters to constrain the model of binary evolution, identify SN Ia progenitors and model the Galactic gravitational wave foreground.
Magnetospheres of Solar System planets	4 Solar system ice/gas planets and their major satellites (~ 20)	Neutral and charged particle dynamics to characterize mass transport.
Circumgalactic medium of galaxies	~ 100 quasars at redshifts greater than 1	Composition and temperature of multiple gas-phases of CGM as constraints on galaxy evolution.
Lyman-alpha forest	~ 10 sightlines	Characterize UV background that keeps intergalactic gas ionized.

2. MISSION DESIGN

Our ESA-M8 mission proposal, Theon, is designed to be consistent with the M-class mission boundary conditions of ESA's call for mission opportunities. Within these limits and, of course, driven by the science goals of the mission and the industrial as well as institutional capabilities of the contributing science consortium partners, we suggest a balanced and cost-efficient mission.

2.1 Boundary conditions

We present the boundary conditions in this chapter, followed by the sizing and configuration argument for our optical telescope assembly (OTA).

2.1.1 ESA's M-class boundary conditions

The most stringent boundary conditions for our mission are set by ESA's call for mission opportunity, in other words, by how ESA defines a medium-class mission.

Mass: The spacecraft dry mass is limited to ≤ 1500 kg.

Launcher: The medium-class mission is planned to be launched using either the Ariane 62/64 or the Vega-C/E launcher. Alternative launch options may be considered if their feasibility can be demonstrated. Non-European launchers procured by ESA are excluded.

Cost: ESA Cost at Completion of ≤ 670 M€ at 2025 economic conditions.

Collaboration: Not strictly a limiting boundary, rather an opportunity encouraged by the call, is ESA's explicit wish to consider strong inter-agency collaboration and contributions from space agencies outside the ESA member states.

Schedule boundaries: Schedule is, of course, also a strong boundary. Components have to be at a certain technical readiness level (TRL) at a certain point in time. Hardware has to be manufactured and tested, etc. So schedules have to be considered from the beginning.

This is of special importance for us also in the sense of the synergies we expect from and for two other space missions. Those will be addressed in more depth in Chapter 2.1.3.

Table 2. Timeline for the M8 mission selection and implementation.

Activity	Tentative dates	Comment
Release of Call	Mar 2025	
Phase-1 M8-proposal submission deadline	May 2025	2 months to submit Phase-1 proposals
Shortlist of proposals retained for Phase-2, M8-proposer notification	Sep 2025	Subset of proposals for Phase-2, following scientific ranking and considering technical and programmatic feasibility
Workshop for Phase-2 proposers	Oct 2025	ESA briefing and one-to-one ESA feedback to proposers. Member States invited to attend
Phase-2 M8 proposal submission deadline	Mar 2026	5 months to submit Phase-2 proposals
Deadline of Letters of Endorsement	May 2026	From Member States and International partners (as relevant)
Completion of evaluation and scientific ranking	Sep 2026	Technical and programmatic feasibility will be evaluated by ESA
Selection of up to five candidate missions for Phase-0 study	Nov 2026	SPC information paper on the selection of the up to five M8 candidates. The selection is made after M7 selection
Down-selection to three candidate missions	Nov 2027	Science program committee (SPC) information paper, following Phase-0 for the five candidates
Selection of the M8 mission	Mar 2030	SPC decision, following the parallel Phase-A studies for the three candidates. Following scientific evaluation and ranking and based on technical and programmatic feasibility, including confirmed support by Member States and International partners (as relevant)
Adoption of the M8 mission	Nov 2032	SPC decision, following Phase-B1
M8 launch	2041	Actual launch date will depend on the selected mission

2.1.2 Scientific boundary conditions

In this paper, we focus on the *exoplanet in transit* science case, as it plays a central role in shaping the early mission and telescope design. The *diffuse medium* case, which will be equally challenging, will be added towards Phase-2 of the mission proposal. For the mission's orbit, the following two main drivers are determining the proposed setup:

Geocorona: The mission must be placed well outside the Earth's exosphere to avoid measurement contamination from absorption or emission caused by our local space environment, the geocorona. As the hydrogen corona extends far beyond the Moon's orbit,²⁵ as measured by the SOHO spacecraft,²⁶ the mission must be located at either the first or second Lagrange point of the Sun-Earth system to mitigate this effect.

Starshade option: In order to be starshade-ready - i.e., prepared for a high-precision formation flight with a large, flower-shaped occulter - it is advantageous to operate at the second Sun-Earth Lagrange point. At L2, the starshade can be positioned so that its backside, facing the receiving Theon telescope, remains permanently in shadow, shielded from direct sunlight. This geometry not only ensures optimal optical performance but also provides a thermally stable environment and minimizes stray light from the Sun.

Considering both mission constraints, the *second Lagrange point* presents the most favorable configuration.

2.1.3 Programmatic boundaries

Theon and Theon* are prepared by the Pathfinder micro-sat mission **BavariAE**.²⁷ A mission based on funding from the state of Bavaria. BavariAE aims to measure chords through the Earth's exosphere and upper atmosphere from a high orbit using the Sun as a source. The Pathfinder mission's data will allow for testing and validation of exoplanet transit observation methods under well-known conditions. It aims for a resolution of $R = 200,000$ and covers the wavelength range from 2000 to 8000 Å, similar to Theon in terms of spectroscopic capabilities. While BavariAE is not setting any schedule constraints on Theon, the goal is to have first commissioning and science verification data from BavariAE available before the final selection of the M8 mission for a Phase-A study. This selection is planned for March 2030 according to Table 2.

Looking beyond the Theon* mission, key technologies - such as the low-resolution rendezvous spectrograph proposed for our ESA's M8 mission, along with the instrumentation for starshade acquisition, communication to the starshade, and closed-loop formation flying with the starshade - can be tested and matured alongside Theon*. This is intended to allow a rendezvous with a starshade also for the Habitable Worlds Observatory. From a broader programmatic perspective, BavariAE can be seen as the precursor preparing the field for Theon,

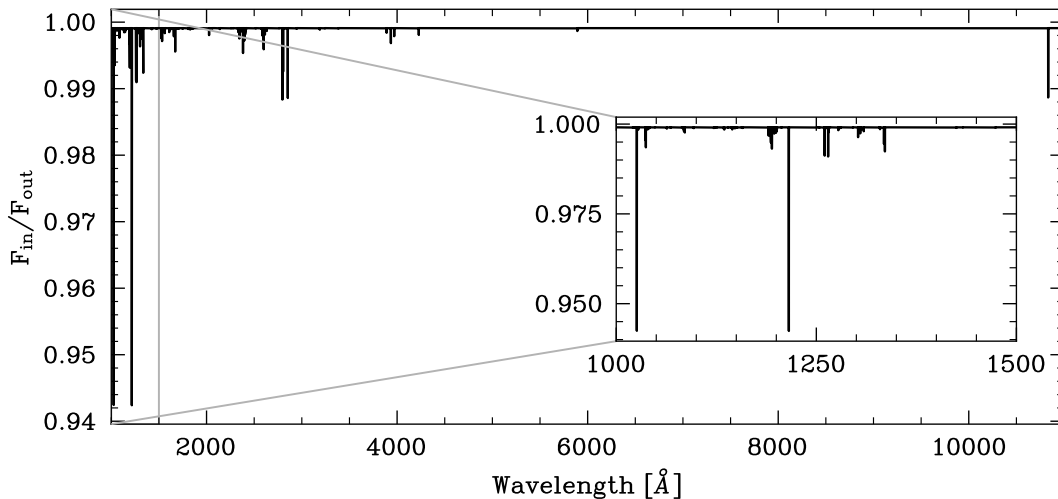


Figure 1. Model spektrum of TOI-2076b in the UV-VIS spectral region.

while Theon - together with its extension Theon* - serves to prepare and de-risk the path toward the ultimate goal: the Habitable Worlds Observatory.

2.2 Sizing the telescope

For Phase-1 of the proposal process (answer to ESA's call for mission opportunity), we perform a preliminary sizing of the mirror based on TOI-2076b: a sub-Neptune with a radius of 2.5 Earth radii, an orbital period of 10.36 days, and a transit duration of 3.25 hours.²⁸ The host star is a K0 main-sequence star with an effective temperature of 5200 K and a metallicity consistent with solar.²⁸ It is located about 42 pc away and has a visual magnitude of $V = 9.24$.²⁹ A transit duration (avoiding ingress and egress) of 2.5 hours is assumed. The goal is to achieve a signal-to-noise of $S/N > 6$, per resolution element, in 5 transits at a wavelength of 3000 Å and at a resolving power $R = 100,000$. For this estimate, we adopt a simulated spectrum spanning 1500 – 9000 Å,³⁰ which yields predicted spectral line depths on the order of 0.1 %. The simulated absorption spectrum is presented in Figure 1. The model is constrained by the limited set of atomic species and transitions included in the computation. Within this framework, typical line depths are about 1 % near 3000 Å and decrease to ~ 0.1 % around 4000 Å.

A model spectrum of TOI-2076 is shown in Figure 2. The model was taken from the PHOENIX model library.³¹ The PHOENIX models do not account for the stellar chromosphere and therefore do not show chromospheric emission and continuum. They are therefore not representative for the region below 2000 Å. A maximum flux of ~ 3200 photons/s/m²/Å is found at the yellow part of the spectrum around 6000 Å. Below 3000 Å, the stellar flux is decreasing quickly by several orders of magnitude. Especially the bound-free absorption edges of Mg, Al, Si, and finally C are dramatically decreasing the flux as we go to smaller wavelengths.

Figure 3 shows the same flux model scaled by a resolution element of $R = 100,000$. Donating on the order of 540 photons per second and 2 m aperture at 6000 Å and 85 photons at 3000 Å. At 2000 Å the stellar flux is already diminished to 1 photon every 10 seconds. The zoom in Figure 3 shows a 100 Å wide window at 2500 Å. The spectrum is full of lines, and no flat continuum is visible in cool star spectra.

While we present the calculation of the proposed telescope and instrument configurations' efficiency in Chapter 3, we show the calculated S/N per resolution element in Figure 4. Detector noise is ignored for this calculation as we are (mainly) in the high photon number case where shot noise described by the Poisson process is dominant.

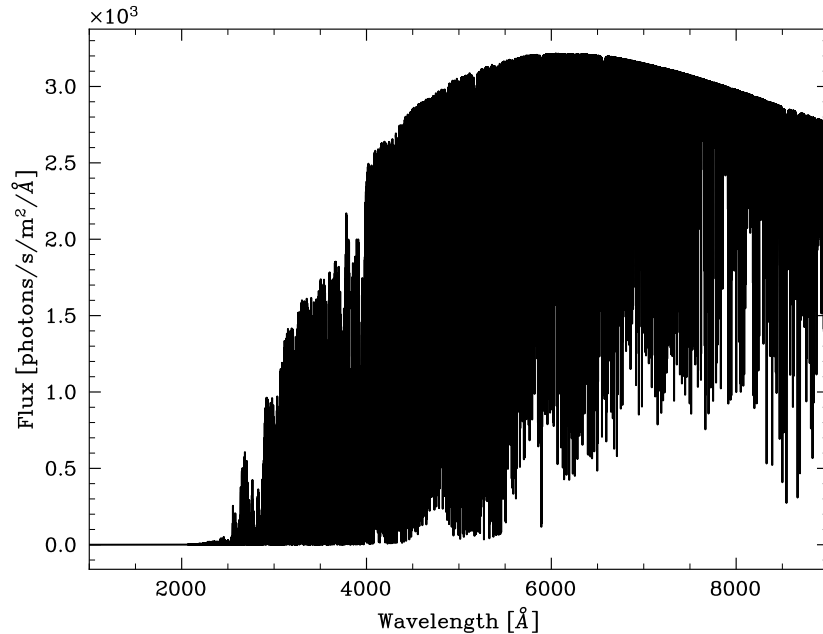


Figure 2. PHOENIX model spectrum of TOI-2076.

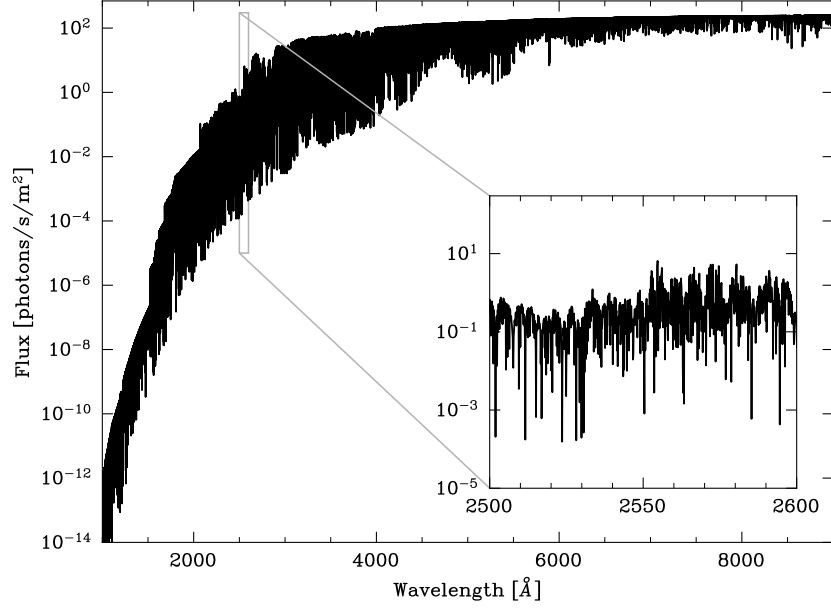


Figure 3. PHOENIX model spectrum of TOI-2076, scaled by a resolution element of $R = 100,000$.

Multiplying flux per resolution element with the assumed (conservative) telescope and spectrograph throughput, we calculate the S/N achieved on a 0.1% deep line within 5 orbits with a length of 2.5 hours each and present the results in Figure 4. The straight red line in Figure 4 shows the $S/N = 6$ limit we set as a preliminary requirement to size the mission aperture. The assumptions for system efficiency were those with an existing, catalogued detector³² (Figure 7 right-hand side). $S/N \geq 6$ is achieved above 2888 Å.

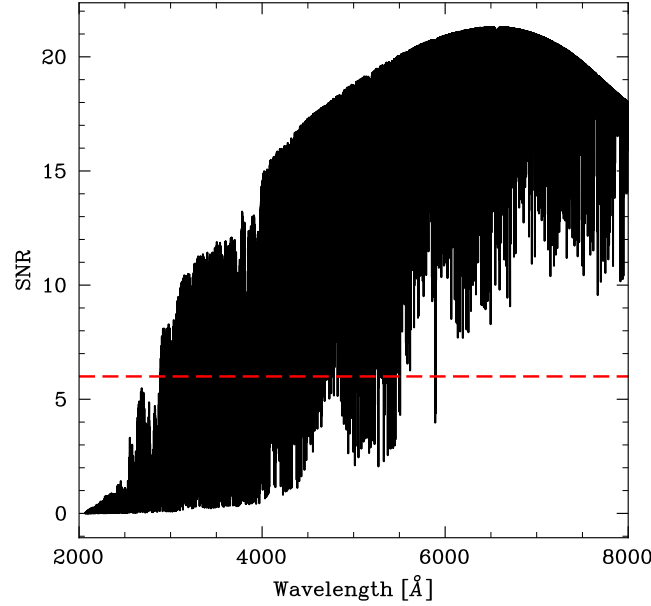


Figure 4. Calculated S/N achieved in 5 orbits of 2.5 hours duration each with a 2 m aperture telescope. The dashed red line marks the $S/N = 6$ threshold, defined as a preliminary requirement for sizing the mission aperture.

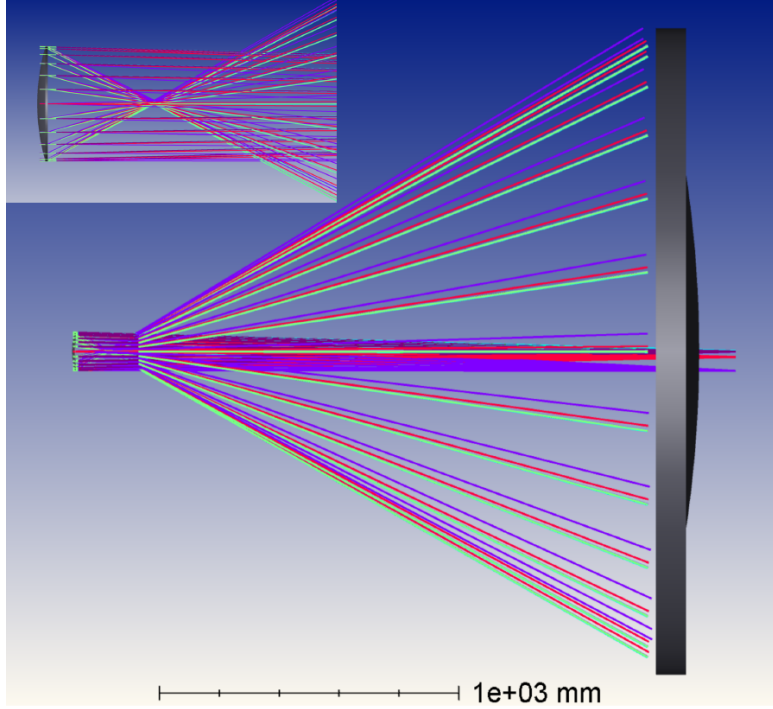


Figure 5. Gregorian 2 m telescope design. M1-M2 distance is 2050 mm. Secondary mirror diameter is 125 mm.

3. TELESCOPE AND INSTRUMENTS

In this chapter, we describe the telescope and instrument configuration planned for Theon. The focus is on the optical configuration, its testing, and its efficiency and robustness.

For Theon*, a *starshade ready package* is briefly described.

For the Phase-1 proposal, we have used simple flat efficiency assumptions over the whole Theon wavelength range. We will show these as a reference and start to add the first “more realistic” data based on existing components in this paper.

The general conceptual idea we follow for the optical telescope assembly is the one described by the existing Hypatia-STOIC study.³³ Utilizing a large, extremely lightweight primary mirror and accounting for zero-gravity residuals by applying in-orbit wavefront correction. The STOIC deformable mirror (DM) is one example of a space-grade deformable mirror that has been studied and developed by the Fraunhofer-Institut für Angewandte Optik und Feinmechanik (IOF) Jena in Germany. It currently has a TRL of 5 in the visible. The German Aerospace Agency DLR is currently funding a full-scale industry study, led by the Theon team in Munich, on the application of this concept to a 2-meter class, Gregorian, UV-visible space telescope. The study schedule is compatible with the Phase-2 proposal timeline and the selection process towards Phase-A.

3.1 The Theon telescope

For Theon and its extension Theon*, a warm (0°C) Gregorian telescope configuration has been selected. The design incorporates the previously determined primary mirror size (see Section 2.2), providing a light-collecting area equivalent to 2.0 m per field point. Figure 5 presents the draft design developed for the Phase-1 response to the call. The compact optical layout, with a distance of only 2050 mm between the primary and secondary mirror, enables an f-number of 18 using a 125 mm diameter secondary mirror.

The choice of a Gregorian design is based on the following arguments:

- Gregorians are relatively easy to align and robust with respect to launch loads and assembly procedures.
- The optical system aperture is located on the secondary mirror, which is therefore the ideal place to correct aberrations. These aberrations that need to be corrected are mainly emerging from residuals of the gravity release that are imperfectly modeled and cannot be fully tested on the ground. These residuals are expected to be non-negligible for an ultra-lightweight telescope, which was shown in the Hypatia/STOIC study. As the telescope operates close to room temperature, we do not expect large residuals between thermal on-ground testing and in-orbit thermal performance.
- The design also allows us to independently test the primary mirror and the path down from the intermediate focus, over the secondary mirror, and to the instruments, by means of computer-generated holograms (CGHs) in the primary focus. The primary mirror and the rest of the system are aligned using CGHs.
- Gregorians show superior baffling and stray light reduction properties. This is especially important for the Theon* application looking at a very dim source next to its host star. The latter still exhibits substantial leakage around the starshade, reaching levels comparable to the brightness of the planetary source.

Besides the stated optical and optomechanical reasons for choosing a Gregorian design, the possibility of splitting the test up- and downstream of the primary focus is of importance. Since the tests are conducted close to room temperature, dividing the system into two “halves” can significantly reduce testing costs while also lowering schedule and program risks.

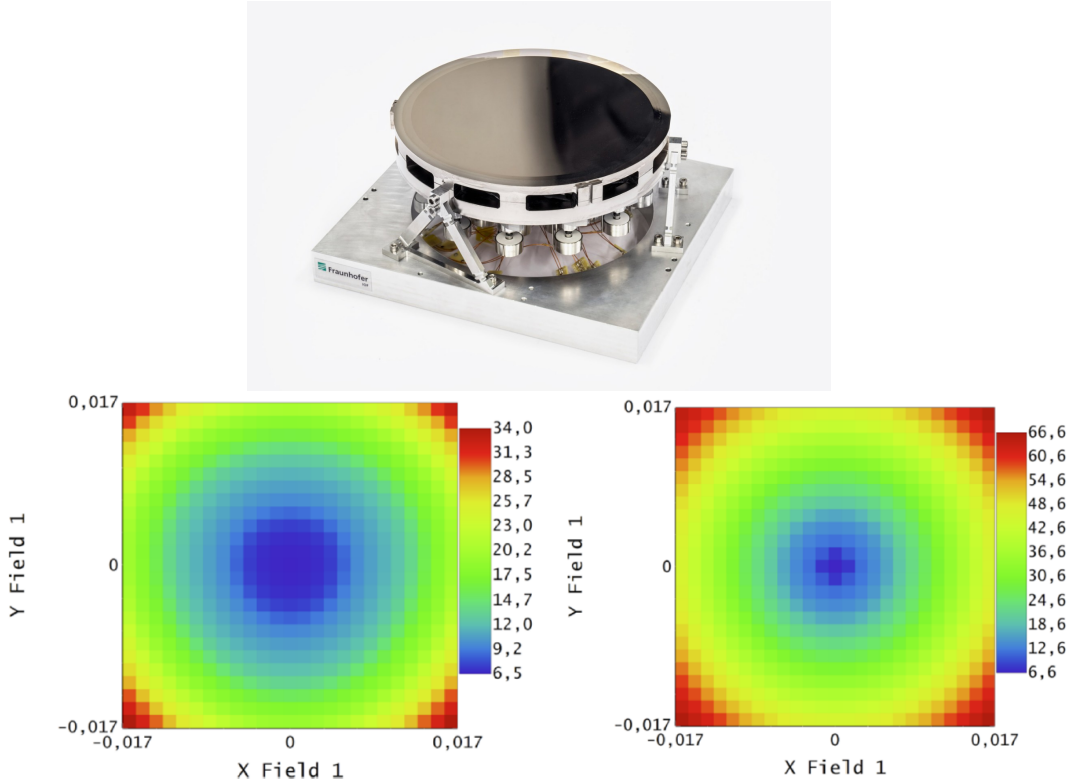


Figure 6. Upper panel: STOIC mirror model at IOF. For visible/IR, the model can be considered TRL5. For UV/visible, TRL3 can be assumed. Lower left: Ideal 80 % encircled energy (EE80) over a 2×2 arcmin FoV. Lower right: EE80 after random distortion of 3 waves on M1 and correction on the secondary mirror.

Please mind the different scales in the lower two plots.

Table 3. Assumptions on telescope and instrument components efficiencies.

M1 reflectivity	0.85	Number of mirrors in instrument	3
M2 reflectivity	0.85	Grating efficiency	0.70
FP-Assembly throughput	0.80	Detector efficiency	0.50
Spectrograph efficiency	0.17	Cross disperser throughput	0.80
Total efficiency	0.10	Total instrument efficiency	0.17

One can even consider encoding effects of refraction (on possible refractive components), as well as temperature effects between room temperature and operational temperature, into the CGHs wavefront. This would allow to (pre-) test the system warm in the lab. The cost and risk reduction implications are obvious.

An active secondary mirror, based on an Euclid-type³⁴ secondary mechanism, is assumed to be similar to what has been developed by IOF Jena for the Hypatia/STOIC study. A first test with deformations up to Zernike coefficients of order 5 (e.g., Pentafoil) has been performed over a 2×2 arcmin field of view (FoV). Two microns of distortion were put on the primary mirror and corrected by an active secondary. This idealized modeling shows that the field center can be corrected well and that the concept holds. Details will be part of the DLR-funded industry study on the feasibility of the 2 m telescope within the M-class framework. Figure 6 shows a model of the STOIC mirror at IOF, the undisturbed image quality, and the image quality after correction. The DM can not only be used to correct the wavefront, but also to adapt the image size to fill the spectrograph's apertures optimally. This is an application of the DM that will be studied together with the feasibility of the telescope concept.

For the Phase-1 proposal, we have used the wavelength-independent assumptions presented in Table 3. Those yield a total telescope plus instrument throughput of $\approx 10\%$.

A first slightly more elaborate efficiency calculation is made based on the conservative, and well understood, Hubble Space Telescope coating.³⁵ A throughput of the focal plane assembly (FP-Assembly), distributing the light to the individual instruments, is assumed to be 80 %. This is conservative for fiber losses and for the likely use of a beam splitter to separate light for acquisition and guiding. The result is shown in Figure 7.

3.2 The TheoN instrument suite

A suite of three science and two technical instruments is foreseen. All science instruments are driven by UV transmission and efficiency.

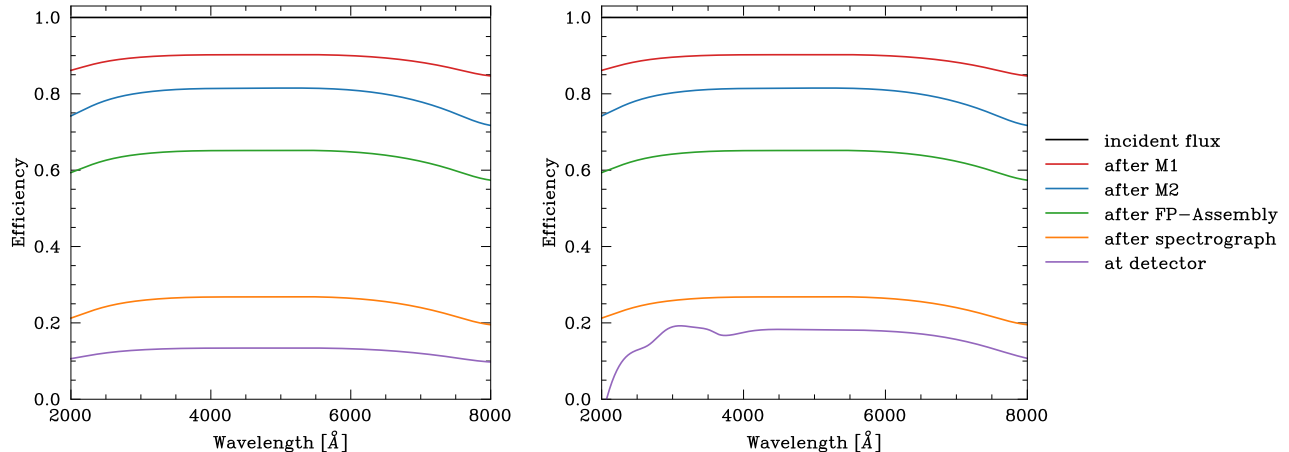


Figure 7. Telescope throughput not taking into account the secondary and spider vignetting.
Left: With 50 % flat quantum efficiency (QE) detector. Right: With an existing delta-doped detector.³²

The instruments planned for Theon and Theon* are:

DUVES, the deep UV Échelle spectrograph: A spectrograph with a resolution of $R = 30,000$ covering the wavelength range from 1000 to 2000 Å. It will be directly coupled to the focal plane to avoid additional bounces or refractive losses. Grating and detector variants are under study. A trade-off between micro-channel plate (MCP) coupled charge-coupled devices (CCDs) and delta-doped silicon detectors will be performed. A compact Échelle spectrograph design using a fused silica prism as a cross-disperser is currently the baseline.

Hires, the optical high-resolution Échelle spectrograph: An Échelle spectrograph ($R = 100,000$) covering the wavelength range from 2000 up to 8000 Å. An extension to 9000 Å is under investigation as a goal. A classical white pupil design is currently the baseline, as this allows efficient grating stray light suppression, especially in the case of bright stellar sources with a high dynamical range from the UV to the VIS spectral range. A fused silica prism will be used as a cross-disperser. Delta-doped and gradient-coated complementary metal-oxide-semiconductor (CMOS) detectors and Échelle gratings with structured grooves to optimize throughput over a wide bandwidth are the current baseline. For CMOS-based detectors, a readout scheme that allows for optimizing integration time for the varying flux of the source is planned.

Fiber-coupling of this instrument is currently under investigation to allow for a relatively simple topology during integration and avoid the need to have several directly coupled instruments in co-focal configurations. Fiber coupling will also allow to test the instrument independent of the telescope and focal plane assembly. Reducing test and integration time, thus reducing risk and cost. Even a short, e.g., octagonal, fiber can also help to scramble the light towards the spectrograph input aperture and allow for a highly stable illumination pattern, allowing for better wavelength calibration and stability.

RSPec, the rendezvous spectrograph: The reflected light science case in the starshade rendezvous scenario requires a highly efficient low-resolution spectrograph. This $R = 5 - 150$ rendezvous spectrograph will cover the wavelength range from 2000 to 8000 Å. Again with a goal of reaching out to the red to 9000 Å. A design with only a single optical element, a convex freeform grating with binary optics characteristics, and structured groove shapes is under investigation. This would allow for maximum throughput and could generate margins for a beam splitter separating out some light for guiding and starshade maneuver flying. Micro-lenses on the detector can help to set the resolution right, especially in the lowest resolution UV part of the spectrum.

AGWCam, the guiding, acquisition, wave-front sensing and rendezvous maneuver camera: This system will work redward or in a selected band within a wavelength range that is less important for the science of the wavelength covered by the instruments. It will offer a pupil imaging mode for starshade formation flying.

SAC, the starshade acquisition camera system: Similar to a star tracker, this system will be used for coarse alignment with the beacon launched by the starshade. The guiding and acquisition camera system will take over once coarse alignment is reached.

Student project: One further instrument, a red light to NIR spectrophotometer with very low resolution of about 20 or less, could be added as a student-provided instrument, giving the mission a large educational aspect. This fiber-coupled instrument would cover the spectral region from 800/900 nm to ~ 1.4 micron. Science-wise, this would allow for a larger overlapping wavelength regime with the James Webb Space Telescope³⁶ (JWST) and the huge ground-based facilities that are to come for infrared astronomy. It would not add any driving requirements and could be replaced by a mass dummy all along the mission's development phases until launch.

Fiber coupling is desired for the HIRES and RSPEC instrument for two reasons:

1. A small Integral Field Unit (IFU) type (5-7 fibers) configuration would allow to measure and subtract solar system and exo-zodiacal and other parasitic light.
2. As for the workhorse HIRES spectrograph, fiber coupling allows the independent test of the instrument before integration to the focal plane, and eases topological issues near the focal plane and when integrating and aligning the instruments.

Redundancy concepts will be examined for all instruments except the far-UV Échelle spectrograph (DUVES). It is considered the most cost-effective way to minimize reliability issues in components such as adhesives and electronics, while ensuring the telescope and its instruments maintain strong long-term performance.

All three science instruments share one focal plane unit, distributing light to the instruments. To keep integration and testing as modular and efficient as possible, two of the instruments (HIRES and RSPEC) are fiber-coupled by short (~ 25 cm) UV-visible grade optical fibers. Including reflection losses at the fiber ends, those fibers will cause $< 15\%$ light losses – about the same amount as a single Hubble-type MgF₂-coated aluminum mirror would cause in the deep UV regime. In this configuration, only DUVES is directly coupled to the focal plane, allowing maximum throughput in the lowest wavelength region that suffers most from additional optical elements. Our goal is to keep detector technologies and readout electronics requirements similar in all UV channels to allow the re-use of concepts and components in the various instruments.

The efficiency of the high-resolution spectrographs HIRES and DUVES is calculated under the following assumptions:

Mirrors: For the 3 mirrors in an Échelle spectrograph, we assume a Hubble-type coating, identical with the one assumed for the telescope itself. As the bandwidth of the instruments is smaller than that of the telescope, more optimized coatings will gain us throughput in future iterations of the design and its evaluation.

Échelle grating: The Échelle gratings efficiency is assumed to be 70 % flat. This is underestimating the peak efficiency and overestimating the rim of the orders. Shaped groove gratings can deliver very broadband high efficiency values. We will definitely consider the use of such gratings in the future.

Detector: Delta-doped CCD and CMOS detectors achieve superior quantum efficiency in the near-UV regime down to at least 200 nm. We are working on detailed models, including gradient coatings on the detectors. For Phase-1 of the proposal, we are using a conservative 50 % flat detector quantum efficiency.

Cross disperser: For the cross disperser, and its anti-reflection coatings, needed in an Échelle spectrograph, in our case, most likely a fused silica prism, we assume a throughput of flat 80 %.

With these assumptions, we achieve a preliminary efficiency as shown in Figure 8. By applying an existing delta-doped detector³² (compare Figure 8 right), we obtain a peak efficiency of 29 % at 3092 Å and an efficiency of 20 % at 2500 Å. The efficiency used for the Phase-1 proposal was assumed to be flat at 17 % (see Table 3).

3.3 The starshade ready package

In the first stage of the proposal process, getting from Theon to Theon* is covered by the NASA-JPL activities to make the Nancy Grace Roman Space Telescope (RST) ready for a starshade rendezvous in the future. This has been in-depth studied by JPL, and we rely on this knowledge that will later be refined and applied to our case.

It is important to notice that Theon* is an addendum to the Theon core mission, which is completely standalone in its scientific value and yield. The mission would benefit tremendously from a starshade, but it would not suffer from the rendezvous not happening.

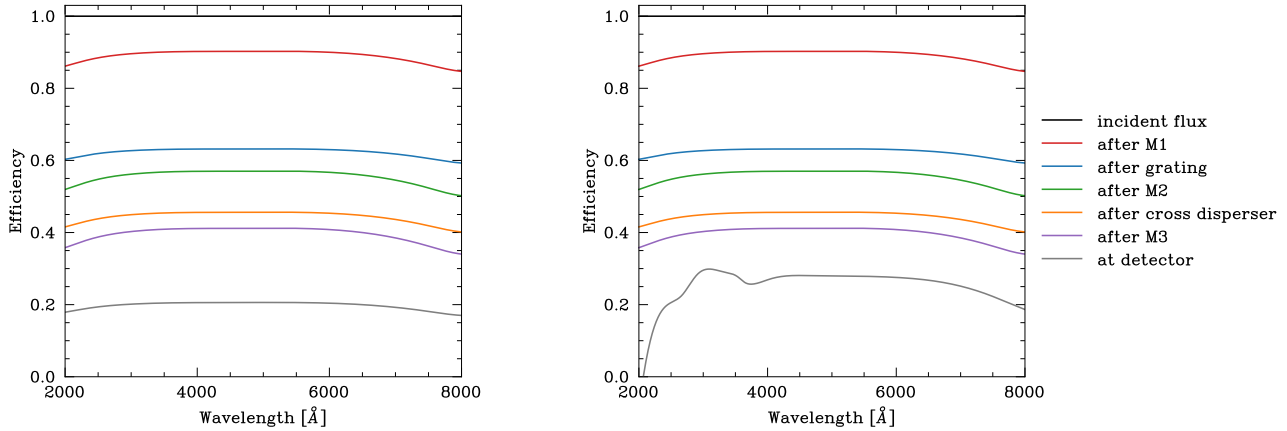


Figure 8. Spectrograph(s) throughput. Left: with 50 % flat QE detector. Right: With an existing delta-doped detector.³²

3.4 Instrument control and data handling

All instruments will need data processing units (DPUs). A global instrument control unit (ICU) will serve as payload control and infrastructure device, providing power for the instruments and heaters, etc. The DPUs and ICU will have active and redundant sides.

A trade-off study will be performed to determine the appropriate level of on-board data processing. As both frame rates and frame sizes for high-resolution Échelle spectroscopy are moderate, a downlink of all compressed raw frames seems feasible. For low-resolution spectroscopy, the spectral information and detector real-estate is even smaller, exposure times are longer, it is therefore likely to download all raw image frames.

Guiding and potential starshade formation flying will require onboard quasi-real-time processing. Again, the relevant part of the detector containing information is limited, therefore, no problems in data storage and handling are expected.

Special operational modes, such as the wave front correction process using the secondary mirrors' active surface, will be done partly in orbit and partly by the operation team on the ground. As this procedure will have to take place mainly during the commissioning phase and a few times along the mission, this is our preferred approach, not relying on fully autonomous systems.

3.5 First budgets

The spacecraft will fly in a Lissajous orbit around the L2 Lagrange point of the Sun-Earth system. The gravity environment of the Earth has to be avoided, and starshade rendezvous maneuvers in other orbits are hardly realistic. L2 is superior to L1 because the Earth and the Sun are aligned, thus avoiding the Earth as a source of light contamination in terms of both reflected light and the Earth's geocorona.

The mission lifetime is assumed to be 6 years (nominal) with 3+3 years of extensions. As we plan to use CMOS detectors, the aging of the detector is easier to cope with than for CCDs. All hardware will be designed to have a possible lifetime of 8 years or more. Consumables will also be budgeted for 8 years of operation. First budgets for Telemetry (TT&C), Altitude Orbital Control System (AOCS), Central Data Management System (CDMS),

Table 4. First estimates for on board budgets.

Abbreviation	Budgeted item	First Estimate excl. Margins
TT&C	Telemetry and Telecommanding	100 GBits/day science 10 Gbits/day commanding and health
AOCS	Attitude Orbit Control System	33 mas
CDMS	Central Data Management System	200 Gbit
EPS	Electrical Power System	115 W
RCS	Reaction Control System	100 kg Hydrazine, 75 kg cold gas

Table 5. First estimates for spacecraft component masses.

Budgeted item	Mass budget	Comment
OTA	500 kg	including support structure
Hires	50 kg	Instrument & warm electronics
DUVES	40 kg	Instrument & warm electronics
RSPEC	10 kg	Instrument & warm electronics
Service module	800 kg	Euclid like ³⁴

Electrical Power System (EPS), and Reaction Control System (RCS) have been estimated and are presented in Table 4. Based on an estimate of 15 kg/m^2 for the aerial density of the primary mirror, an OTA mass of 10 times the primary mass was estimated to be approximately 500 kg. Instrument masses are estimated in Table 5.

The most critical budget is clearly the OTA itself. Its feasibility is the key point of the mission. We have records of 2 m class silicon carbide (SiC) telescopes with similar optical configurations that have OTA masses below 400 kg. This possible supplier estimated the mass of the OTA and the back structure for our current draft design to be 382 kg. This leads to $> 20\%$ margin with respect to the 500 kg assumption taken in Table 5.

4. THEON IN THE MISSION LANDSCAPE

Theon and Theon* are not alone out there. Many successful science missions are in operation or programmed, and many are undergoing a proposal or selection process. In this chapter, we will briefly discuss synergies, competitions, and paths that can lead to greater science enabled by Theon and Theon* embedded in the complex and heterogeneous landscape of space and ground-based projects.

4.1 Mission landscape

With the Hubble Space Telescope nearing the end of its decades-long successful orbital life, space-based UV high-resolution spectroscopy will not be possible any longer. We will therefore lose an important wavelength regime for exploring the universe.

At the same time, huge ground-based facilities like the European Southern Observatory's (ESO) Extremely Large Telescope (ELT) are planned to see first light in the early 2030s. This will allow more survey work to be performed by the then *second largest* sized telescopes like the four Very Large Telescope (VLT) units, the Subaru telescope, the Keck telescopes, or the Gran Telescopio Canarias (GTC).

The importance of maintaining access to the UV window is demonstrated by the multitude of small missions that have been proposed by several space agencies across the world. The Indian space agency is planning the INSIST³⁷ mission. NASA is launching the UVEX³⁸ mission, which is an all-sky survey of galaxies and transients. The Israeli space agency has approved the launch of the ULTRASAT³⁹ mission in 2026, which will mainly study gravitational wave sources and high-energy astrophysical phenomena. The Canadian mission CASTOR⁴⁰ is scheduled for launch in the late 2020s with a broad slate of science cases. All of these mission concepts have mirror sizes of about 1 m or smaller and spectral resolutions of ~ 1000 or less.

And, for high-resolution UV-spectroscopy and exoplanet science, NASA's flagship mission Habitable Worlds Observatory is in its early definition phase, aiming for a Mission Concept Review (MCR) in 2029.

Our mission proposal, with its launch in 2041, fits nicely in the gap between the small aperture photometric missions and the HWO flagship that shall be launched in 2045.^{2,3}

Another mission that is most likely re-proposed for ESA's M8 call, and that was proposed for M5 and M7 already before, is the French-led Arago⁴¹ mission concept. Arago proposes UV spectropolarimetry with a resolving power of at least $\sim 10,000$ paired with a 1 m mirror. The multi-reflection optical design of Arago required to achieve polarimetric capability necessarily reduces the sensitivity of the instrument to fainter exoplanet host stars, protoplanetary disks, and extragalactic sightlines. To fulfill our scientific goals, a resolving power of $\sim 100,000$ and a larger mirror size (2 meters) of Theon are necessary. It is important to note that the Theon mission does not perform polarimetry, only spectroscopy.

For the synergies with already flying or programmed missions, we want to highlight the successful TESS⁴² and almost ready to be launched Plato⁴³ missions that are perfect target finders for the exoplanet science of Theon and Theon*. The Ariel⁴⁴ mission that will characterize a large number of transiting exoplanets in low resolution and is planned to be launched in 2029, will help to further characterize and select the best targets for Theon and Theon*. Last but absolutely not least, the JWST³⁶ is able to do infrared low- to mid-resolution spectroscopy of exoplanet targets. And it is a perfect complement to the UV capabilities that Theon and Theon* will offer.

Leaving the field of exoplanet science, the eROSITA⁴⁵ and Athena⁴⁶ missions delivered and will deliver excellent data and objects that need UV high-resolution complementary data.

4.2 Starshade considerations

Using basic starshade scaling relations¹ from a starshade that has a total diameter of 60 m tip-to-tip for a 6 m class HWO concept covering the wavelength from 500 to 1000 nm reduces in size significantly for a 2 m UV-VIS telescope.

A rendezvous starshade for Theon* at a wavelength of 250-600 nm would have a tip-to-tip size of the order of 20 m. If one restricts the red cutoff of the wavelength range closer to the UV, the starshade could be even smaller. Still a large structure out in space, but significantly less complex and risky in most aspects of starshade design and deployment.

Maneuver flying will remain challenging to a level that is similar to the HWO case, but with the LISA⁴⁷ space interferometer being developed currently by ESA, this aspect can be considered solved technically by the time M8 Theon will be launched. The technology of starshade formation flying is also developed at JPL and has reached TRL5.⁴⁸

4.3 An evolutionary path to habitable worlds

In the landscape laid out above, Theon and its rendezvous extension Theon* can be seen as a sequence or path of missions:

1. BavariAE will enable us to validate our models and improve our understanding of the Earth's exosphere and of reflection spectroscopy from the Earth's surface in an almost laboratory clean way. With its spectral resolution of about twice the one desired for Theon, it will allow to verify the resolution "really needed" for exoplanet spectroscopy.
2. Theon and Theon* will allow a large variety of science explorations in the post-Hubble era. For the defining science case of exoplanet transit spectroscopy, it will explore a large variety of planets down to super-Earths. For reflection spectroscopy using a starshade and a highly efficient low-resolution spectrograph optimized for this science, it will explore not only a number of Earth-sized planets but also mark an important step on the way to the Habitable Worlds Observatory. Flying about 1/2 decade prior to HWO starshade technology, the rendezvous spectrograph and mission parameters can be matured, and the starshade for HWO de-risked dramatically. This, with a starshade only one third of the diameter and one tenth of the area as the one needed for HWO later.
3. The Habitable Worlds Observatory, envisioned as the ultimate flagship for exploring Earth-like exoplanets, could build upon RSPEC and the design, implementation, and operational lessons learned from Theon*. RSPEC could effectively serve as a blueprint for a low-resolution spectrograph for HWO.

5. SUMMARY AND CONCLUSION

We have presented a mission concept and early design considerations for a 2-meter class UV-VIS space observatory concentrating on high-resolution spectroscopy. An extremely lightweight telescope is needed that will most likely require in-orbit wave front correction by a deformable mirror. We base an ongoing industry study for the feasibility of this concept on the Hypatia & STOIC study.³³

All five instruments, three science instruments and two technical instruments, are optimized for high UV throughput and implement concepts that allow for independent instrument test and not overly complex integration to the spacecraft's payload module. We try to keep detector technologies and readout electronics requirements similar in all UV and UV-VIS channels to allow the re-use of concepts and components in the various instruments. The option of flying a sixth instrument, a student project designed and built, a red light to NIR spectrophotometer is kept, but only sets goals and has no requirements for the mission components.

For the Phase-1 answer to ESA's call, we used very conservative assumptions on throughput and detector efficiency. With this paper, we present one step in the direction of more realistic, yet safe, assumptions. We find a total efficiency of our system of $\leq 15\%$ between 2800 and 6500 Å. Compared to the well explored efficiency of Hubble's STIS instrument in the H230 grating configuration, which has a peak efficiency of 0.5 % and goes down to 0.2 % at 3000 Å, we suggest to have a 25 to 60 times higher throughput. Combined with the much longer simultaneous wavelength coverage, we increase observation efficiency by a factor of significantly more than 100.

To current knowledge, the mission is feasible, scientifically highly beneficial, and it closes the gap that Hubble will leave when decommissioned. As currently around 40 % of Hubble's time goes into UV high- and medium-resolution spectroscopy, keeping this gap open would be highly detrimental for the scientific community.

5.1 Programmatic longer term view on Theon and Theon*

On a longer time scale and broader mission landscape view, Theon and Theon* with the RSPEC spectrograph and the technical rendezvous instrumentation package would not only be a great exoplanet transmission spectroscopy facility, but also a mighty step-stone on the way to starshade-supported exoplanet research with future large-scale facilities such as the Habitable Worlds Observatory.

As the knowledge to design and manufacture starshades is present at JPL^{49,50} and Northrop Grumman,^{51,52} it is time to do one. And why not start with a 20 m starshade that is significantly smaller and needs a much less powerful bus than the one for a 40 – 60 m class HWO starshade.

HWO does not need the Nancy Grace Roman space telescope⁵³ and its technology demonstrator coronagraph (CGI) to be successful. But with the prospective success of the Roman mission and its tech demo, confidence that this can be done for HWO as well will increase substantially.

Theon* and its low-resolution rendezvous spectrograph can be the demonstrator and learning-how-to-do-things engine for starshades, as Roman and CGI are for coronagraphy.

Theon and Theon*: What UV is what you see.

ACKNOWLEDGMENTS

Thanks to our colleagues at JPL, namely Shouleh Nikzad, Robert O. Green, Mark R. Swain, Charles Lawrence, Kendra Short, and Bertrand Mennesson for helpful discussions and technical as well as administrative insights.

Special thanks also go to Prof. Ralf Bender for his support through knowledge, advice, and for funding a position to get this mission preparation work done.

Thanks go to the German Aerospace Agency DLR for prospective funding under grant 50OO2520. Special thanks in this context also go to Anke Pagels-Kerp, Alessandra Roy and Eberhard Bachem from DLR. They initiated the process of “proposing a mission from Munich” more than 2 years ago and continuously supported our ideas.

REFERENCES

- [1] Arenberg, J. W., Harness, A. D., Jensen-Clem, R. M., “Special Section on Starshades: Overview and a Dialogue,” *Journal of Astronomical Telescopes, Instruments, and Systems* **7**(2), 021201 (2021).
- [2] Dressing, C., Ansdell, M., Crooke, J., Feinberg, L., Mennesson, B., O’Meara, J., Pepper, J., Roberge, A., Ziemer, J., Habitable Worlds Observatory Start, T., et al., “The Habitable Worlds Observatory: Status, Plans, and Opportunities,” in [American Astronomical Society Meeting Abstracts], *American Astronomical Society Meeting Abstracts* **244**, 210.04 (June 2024).

- [3] Roederer, I. U., Ezzeddine, R., Sobeck, J. S., “Habitable Worlds Observatory: The Nature of the First Stars,” (2025).
- [4] Endelman, L. L., “Hubble space telescope: mission, design, problems, and solutions,” in [*21st International Congress on: High-Speed Photography and Photonics*], **2513**, 1204 – 1217, International Society for Optics and Photonics, SPIE (1995).
- [5] Fulton, B. J., Petigura, E. A., “The California-Kepler Survey. VII. Precise Planet Radii Leveraging Gaia DR2 Reveal the Stellar Mass Dependence of the Planet Radius Gap,” **156**, 264 (Dec. 2018).
- [6] Redfield, S., Linsky, J. L., “Evaluating the Morphology of the Local Interstellar Medium: Using New Data to Distinguish between Multiple Discrete Clouds and a Continuous Medium,” **812**, 125 (Oct. 2015).
- [7] Sheffer, Y., Rogers, M., Federman, S. R., Abel, N. P., Gredel, R., Lambert, D. L., Shaw, G., “Ultraviolet Survey of CO and H₂ in Diffuse Molecular Clouds: The Reflection of Two Photochemistry Regimes in Abundance Relationships,” **687**, 1075–1106 (Nov. 2008).
- [8] Frisch, P. C., Redfield, S., Slavin, J. D., “The Interstellar Medium Surrounding the Sun,” **49**, 237–279 (Sept. 2011).
- [9] France, K., Herczeg, G. J., McJunkin, M., Penton, S. V., “CO/H₂ Abundance Ratio $\approx 10^{-4}$ in a Protoplanetary Disk,” **794**, 160 (Oct. 2014).
- [10] Team, T. L., “The LUVOIR Mission Concept Study Final Report,” (2019).
- [11] Jenkins, E. B., “A Unified Representation of Gas-Phase Element Depletions in the Interstellar Medium,” **700**, 1299–1348 (Aug. 2009).
- [12] De Cia, A., Jenkins, E. B., Fox, A. J., Ledoux, C., Ramburuth-Hurt, T., Konstantopoulou, C., Petitjean, P., Krogager, J.-K., “Large metallicity variations in the Galactic interstellar medium,” *Nature* **597**, 206–208 (Sep. 2021).
- [13] Eldridge, J. J., Stanway, E. R., “New Insights into the Evolution of Massive Stars and Their Effects on Our Understanding of Early Galaxies,” **60**, 455–494 (Aug. 2022).
- [14] Sana, H., de Mink, S. E., de Koter, A., Langer, N., Evans, C. J., Gieles, M., Gosset, E., Izzard, R. G., Le Bouquin, J. B., Schneider, F. R. N., “Binary Interaction Dominates the Evolution of Massive Stars,” *Science* **337**, 444 (July 2012).
- [15] Ivanova, N., Justham, S., Chen, X., De Marco, O., Fryer, C. L., Gaburov, E., Ge, H., Glebbeek, E., Han, Z., Li, X. D., et al., “Common envelope evolution: where we stand and how we can move forward,” **21**, 59 (Feb. 2013).
- [16] Belloni, D., Schreiber, M. R., “Formation and Evolution of Accreting Compact Objects,” in [*Handbook of X-ray and Gamma-ray Astrophysics*], 129 (2023).
- [17] Napiwotzki, R., Karl, C. A., Lisker, T., Catalán, S., Drechsel, H., Heber, U., Homeier, D., Koester, D., Leibundgut, B., Marsh, T. R., et al., “The ESO supernovae type Ia progenitor survey (SPY) - The radial velocities of 643 DA white dwarfs,” *AA* **638**, A131 (2020).
- [18] Nelemans, G., “The Galactic gravitational wave foreground,” *Classical and Quantum Gravity* **26**, 094030 (Apr. 2009).
- [19] Amaro-Seoane, P., Andrews, J., Arca Sedda, M., Askar, A., Baghi, Q., Balasov, R., Bartos, I., Bavera, S. S., Bellovary, J., Berry, C. P. L., et al., “Astrophysics with the Laser Interferometer Space Antenna,” *Living Reviews in Relativity* **26**, 2 (Dec. 2023).
- [20] Maiolino, R., Mannucci, F., “De re metallica: the cosmic chemical evolution of galaxies,” **27**, 3 (Feb. 2019).
- [21] Péroux, C., Howk, J. C., “The Cosmic Baryon and Metal Cycles,” **58**, 363–406 (Aug. 2020).
- [22] Tumlinson, J., Peebles, M. S., Werk, J. K., “The Circumgalactic Medium,” *Annual Review of Astronomy and Astrophysics* **55**, 389–432 (Aug. 2017).
- [23] Linsky, J. L., Tripp, T. M., Redfield, S., France, K., “The Case for High Resolution Spectroscopy in the Ultraviolet,” (2025).
- [24] Faucher-Giguère, C.-A., “A cosmic UV/X-ray background model update,” **493**, 1614–1632 (Apr. 2020).
- [25] Baliukin, I. I., Bertaux, J. L., Quémerais, E., Izmodenov, V. V., Schmidt, W., “SWAN/SOHO Lyman- α Mapping: The Hydrogen Geocorona Extends Well Beyond the Moon,” *Journal of Geophysical Research (Space Physics)* **124**, 861–885 (Feb. 2019).

- [26] Guyenne, T. D., ed., [*The SOHO mission : scientific and technical aspects of the instruments*], *ESA Special Publication* **0379** (Jan. 1989).
- [27] Grupp, F., Heng, K., Green, R. O., Hu, R., Kellermann, H., Lamprecht, H., Nikzad, S., “BavariAE: the Earth’s atmosphere and exosphere explored by a micro-sat in the UV-VIS spectral region,” *Manuscript in preparation* (2025).
- [28] Osborn, H. P., Bonfanti, A., Gandolfi, D., Hedges, C., Leleu, A., Fortier, A., Futyan, D., Gutermann, P., Maxted, P. F. L., Borsato, L., et al., “Uncovering the true periods of the young sub-Neptunes orbiting TOI-2076,” *AA* **664**, A156 (2022).
- [29] Høg, E., Fabricius, C., Makarov, V. V., Urban, S., Corbin, T., Wycoff, G., Bastian, U., Schwerkendiek, P., Wicenec, A., “The Tycho-2 catalogue of the 2.5 million brightest stars,” *355*, L27–L30 (Mar. 2000).
- [30] Linssen, D. C., Oklopčić, A., “Expanding the inventory of spectral lines used to trace atmospheric escape in exoplanets,” *Astronomy amp; Astrophysics* **675**, A193 (July 2023).
- [31] Husser, T.-O., Wende-von Berg, S., Dreizler, S., Homeier, D., Reiners, A., Barman, T., Hauschildt, P. H., “A new extensive library of PHOENIX stellar atmospheres and synthetic spectra,” *Astronomy amp; Astrophysics* **553**, A6 (Apr. 2013).
- [32] Teledyne-e2v, “CCD275-42 NIMO Back Illuminated High Performance CCD Sensor,” (2018).
- [33] Devaney, N., Reinlein, C., Lange, N., Goy, M., Goncharov, A., Hallibert, P., MacEwen, H. A., Fazio, G. G., Lystrup, M., Batalha, N., Siegler, N., Tong, E. C., eds., **9904**, 990469, International Society for Optics and Photonics, SPIE (2016).
- [34] Euclid Collaboration, Mellier, Y., Abdurro’uf, Acevedo Barroso, J. A., Achúcarro, A., Adamek, J., Adam, R., Addison, G. E., Aghanim, N., Aguena, M., et al., “Euclid: I. Overview of the Euclid mission,” *697*, A1 (May 2025).
- [35] Quijada, M. A. personal communication.
- [36] Gardner, J. P., Mather, J. C., Clampin, M., Doyon, R., Greenhouse, M. A., Hammel, H. B., Hutchings, J. B., Jakobsen, P., Lilly, S. J., Long, K. S., et al., “The James Webb Space Telescope,” *123*, 485–606 (Apr. 2006).
- [37] Sriram, S., Valsan, V., Subramaniam, A., Unni, C. V., Maheswar, G., Chand, T., “Indian spectroscopic and imaging space telescope (INSIST): An optics design trade-off study,” *Journal of Astrophysics and Astronomy* **44**, 55 (Dec. 2023).
- [38] Kulkarni, S. R., Harrison, F. A., Grefenstette, B. W., Earnshaw, H. P., Andreoni, I., Berg, D. A., Bloom, J. S., Cenko, S. B., Chornock, R., Christiansen, J. L., et al., “Science with the Ultraviolet Explorer (UVEX),” (2023).
- [39] Ben-Ami, S., Shvartzvald, Y., Waxman, E., Netzer, U., Yaniv, Y., Algranatti, V. M., Gal-Yam, A., Lapid, O., Ofek, E., Topaz, J., et al., den Herder, J.-W. A., Nikzad, S., Nakazawa, K., eds., **12181**, 1218105, International Society for Optics and Photonics, SPIE (2022).
- [40] Amenouche, M., Côté, P., Lokhorst, D., den Herder, J.-W. A., Nikzad, S., Nakazawa, K., eds., **13093**, 130933L, International Society for Optics and Photonics, SPIE (2024).
- [41] Muslimov, E., Neiner, C., Minoglou, K., Karafolas, N., Cugny, B., eds., **12777**, 127774F, International Society for Optics and Photonics, SPIE (2023).
- [42] Ricker, G. R., Winn, J. N., Vanderspek, R., Latham, D. W., Bakos, G. , Bean, J. L., Berta-Thompson, Z. K., Brown, T. M., Buchhave, L., Butler, N. R., et al., “Transiting Exoplanet Survey Satellite,” *Journal of Astronomical Telescopes, Instruments, and Systems* **1**, 014003 (Oct. 2014).
- [43] Rauer, H., Aerts, C., Cabrera, J., Deleuil, M., Erikson, A., Gizon, L., Goupil, M., Heras, A., Walloschek, T., Lorenzo-Alvarez, J., et al., “The PLATO mission,” *Experimental Astronomy* **59**, 26 (June 2025).
- [44] Tinetti, G., Eccleston, P., Lueftinger, T., Salvignol, J.-C., Fahmy, S., Alves de Oliveira, C., “Ariel: Enabling planetary science across light-years,” in [*European Planetary Science Congress*], EPSC2022-1114 (Sept. 2022).
- [45] Predehl, P., Andritschke, R., Arefiev, V., Babushkin, V., Batanov, O., Becker, W., Böhringer, H., Bogomolov, A., Boller, T., Borm, K., et al., “The eROSITA X-ray telescope on SRG,” *Astronomy amp; Astrophysics* **647**, A1 (Feb. 2021).

- [46] Nandra, K., Barret, D., Barcons, X., Fabian, A., den Herder, J.-W., Piro, L., Watson, M., Adami, C., Aird, J., Afonso, J. M., et al., “The Hot and Energetic Universe: A White Paper presenting the science theme motivating the Athena+ mission,” (2013).
- [47] Amaro-Seoane, P., Audley, H., Babak, S., Baker, J., Barausse, E., Bender, P., Berti, E., Binetruy, P., Born, M., Bortoluzzi, D., et al., “Laser Interferometer Space Antenna,” (2017).
- [48] Flinois, T., Bottom, M., Martin, S., Scharf, D., Davis, M. C., Shaklan, S., “S5: Starshade technology to TRL5 Milestone 4 Final Report: Lateral formation sensing and control,” *Jet Propulsion Laboratory Publications* (2018).
- [49] Willems, P., Lisman, D., “NASA’s starshade technology development activity,” *Journal of Astronomical Telescopes, Instruments, and Systems* **7**(2), 021203 (2021).
- [50] Damiano, M., Shaklan, S., Hu, R., Dunne, B., Tanner, A., Nida, A., Carson, J. C., Hildebrandt, S. R., Lisman, D., “Starshade Exoplanet Data Challenge: What We Learned,” (2024).
- [51] Samuele, R., Varshneya, R., Johnson, T. P., Johnson, A. M. F., Glassman, T., Oschmann, Jr., J. M., Clampin, M. C., MacEwen, H. A., eds., *Society of Photo-Optical Instrumentation Engineers (SPIE) Conference Series* **7731**, 773151 (July 2010).
- [52] Samuele, R., Glassman, T., Johnson, A. M. J., Varshneya, R., Shipley, A., Shaklan, S. B., ed., *Society of Photo-Optical Instrumentation Engineers (SPIE) Conference Series* **7440**, 744004 (Aug. 2009).
- [53] Bailey, V. P., Bendek, E., Monacelli, B., Baker, C., Bedrosian, G., Cady, E., Douglas, E. S., Groff, T., Hildebrandt, S. R., Kasdin, N. J., et al., “Nancy Grace Roman Space Telescope Coronagraph Instrument Overview and Status,” (2023).